Hindawi
Advances in Materials Science and Engineering
Volume 2018, Article ID 4254156, 6 pages
https://doi.org/10.1155/2018/4254156

Research Article

Transition of Dislocation Structures in Severe Plastic Deformation and Its Effect on Dissolution in Dislocation Etchant

Muhammad Rifai,[1] **Ebad Bagherpour**,[2] **Genki Yamamoto**,[3] **Motohiro Yuasa**,[1] **and Hiroyuki Miyamoto**[1]

[1]*Department of Mechanical Engineering, Doshisha University, Kyoto, Japan*
[2]*Department of Materials Science and Engineering, School of Engineering, Shiraz University, Shiraz, Iran*
[3]*Graduate School of Science and Engineering, Doshisha University, Kyoto, Japan*

Correspondence should be addressed to Muhammad Rifai; rmuhamma@mail.doshisha.ac.jp

Received 27 September 2017; Revised 11 December 2017; Accepted 18 December 2017; Published 30 January 2018

Academic Editor: Alicia E. Ares

Transition of dislocation structures in ultrafine-grained copper processed by simple shear extrusion (SSE) and its effects on dissolution were manifested by simple immersion tests using a modified Livingston dislocation etchant, which attacks dislocations and grain boundaries selectively. The SSE process increased the internal strain evaluated by X-ray line broadening analysis until eight passes but decreased it with further extrusion until twelve passes. The weight loss in the immersion tests reflected the variation in the internal strain: namely, it increased until eight passes and then decreased with further extrusion to twelve passes. Taking our previous report on microstructural observation into account, it is suggested that variation in the internal strain is caused by both the variation in dislocation density and structural change of grain boundaries from equilibrium to nonequilibrium states or vice versa. Decreased dislocation density and structural change back to equilibrium state of grain boundaries in very high strain range by possibly dynamic recovery as pointed out by Dalla Torre were validated by X-ray and dissolution in the modified Livingston etchant in addition to the direct observation by TEM reported in our former report.

1. Introduction

Grain refinement to grain sizes below 1 μm by severe plastic deformation (SPD) is now well known for improving strength of bulk metallic materials for structural application [1]. Simple shear extrusion (SSE) technique is one of the SPD methods wherein deformation proceeds by pressing the material through a die with a specifically created direct extrusion path [2]. SSE as well as other SPD techniques represented by equal-channel angular pressing (ECAP) and accumulative roll bonding (ARB) produces ultrafine grain (UFG) materials with residual dislocation inside grains, which may cause unique physical and mechanical properties [3]. Dislocation density increases to the order of 10^{15} m^{-2} with increasing number of passes in SPD, forming finally the so-called deformation-induced grain boundaries with some dislocations remained inside grains. However, we reported in the previous study that the softening occurred with further passes after UFG formation in pure copper processed by SSE, and this softening was considered as a result of a decrease in dislocation density, which was revealed by scanning transmission electron microscope (STEM). This decrease in dislocation density after UFG formation may be caused by the dynamic recovery [3–5]. As a classic approach, a dislocation etchant has been used to locate discrete dislocations and its density in low plastic strain [6]. However, it was reported that the dissolution rate in a modified solution becomes sensitive to dislocation density in very high range and grain boundaries state with residual dislocations after SPD, and the dissolution rate was changed by the flush annealing in spite that grain size is not changed [4, 7]. This study was carried out in order to evaluate dislocation density in very high strain range using a modified Livingston etchant which is very sensitive to dislocations and to examine the dissolution behavior of UFG copper.

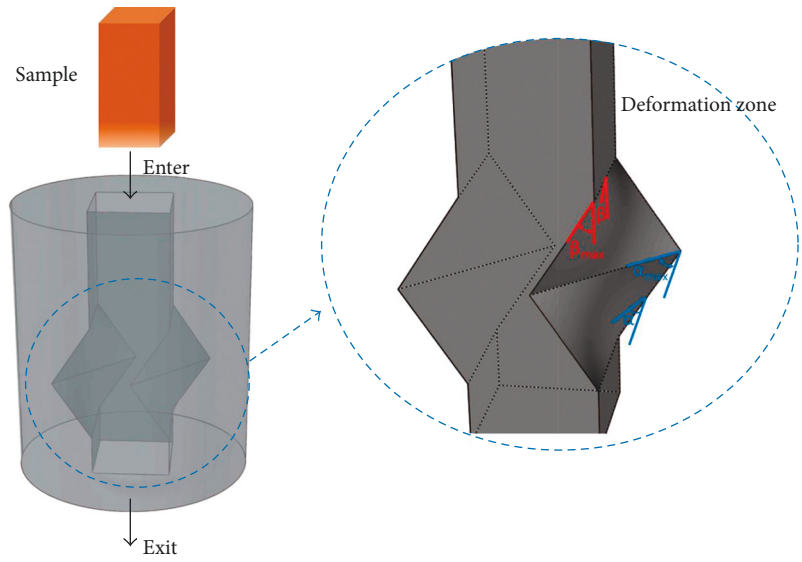

Figure 1: Schematic presentation of the SSE channel.

2. Experimental Procedure

2.1. Simple Shear Extrusion (SSE). A schematic representation of the SSE channel is shown in Figure 1 [3]. Through the deformation channel, the shear strain is gradually applied to the material while its cross-sectional area remains constant [2]. The direction of the shear is reversed at the middle of the channel where the specimen distorts with a maximum distortion angle of α_{max}. Another parameter of SSE processing is the inclination angle (β), which exerts a profound effect on the deformation zone, strain rate, and the load of the process [2, 3, 8, 9]. The SSE can be conducted with a lower cost of production and easier installation than many other SPD methods owing to the straight movement of the billets through the channel.

A bisection die with the maximum distortion angle (α_{max}) and the maximum inclination angle (β_{max}) of 45° and 22.2°, respectively, was designed and constructed, which applies an equivalent strain of 1.155 per pass, as shown in Figure 1 [3]. The deformation channel's cross section is a square with the side of 10 mm. The copper billets of commercial purity with a dimension of 10 mm × 10 mm × 50 mm were machined, annealed for 2 h at 923 K in argon atmosphere and then furnace cooled to room temperature as an initial material. A screw press with a ram speed of 0.2 mm/s was used for SSE processing, namely, route C where the sample is rotated in the same view by 180° between each pass was used for repeating SSE. The initial materials were subjected to two, four, eight, and twelve passes of SSE (see [3] for further details of SSE).

2.2. Microstructural Characterization. The microstructure of samples after two, four, eight and twelve passes of SSE was observed using a transmission electron microscope (JEM-2100F, JEOL) with an acceleration voltage of 200 kV. All the TEM specimens were prepared from extrusion direction (ED) section of the samples. The surface of the specimens was mechanically grounded to the thickness of 100 μm using a SiC abrasive paper. Then, the TEM specimens were thinned by a twin-jet polisher Tenupol 5 (Struers Co., Ltd.) at an applied voltage of 10 V in a mixture of 250 ml ethanol, 500 ml phosphoric acid, 50 ml propanol, and 5 g urea at 273 K until perforation. After that, the specimens were finally polished by an ion beam using the Gatan 691 precision ion polishing system.

2.3. X-Ray Diffraction. The measurement of X-ray diffraction (XRD) on the SSE-processed sample was conducted by the SmartLab, Rigaku. The integral breadth was determined after appropriate fitting of the scattered XRD pattern. The broadening in XRD data line consists of contributions due to coherent domain size, D, and microstrain, ε [10]. The following equation was used to separate the contributions from each other for calculating the dislocation density ρ [10]:

$$\left(\frac{\beta\cos\theta}{\lambda}\right)^2 = \left(\frac{1}{D}\right)^2 + \left(\frac{4\varepsilon\sin\theta}{\lambda}\right)^2, \quad (1)$$

where β is the value of the integral breadth (in radians), θ is Bragg's diffraction angle, and λ is the wavelength of the X-ray beam (Å).

Several XRD peaks of high intensity ($2\theta = 30$–$130°$) were taken, and the plot of $(\beta\cos\theta/\lambda)^2$ versus $(\sin\theta/\lambda)^2$ was constructed [10]. The plots D and ε were calculated using intercept $= 1/D^2$ and slope $= 16\varepsilon^2$. Then, the dislocation density can be calculated from D and ε, with η = integer number, as [10] follows:

$$\rho_D = \frac{3\eta}{D^2} \text{ with } \eta = 1, \quad (2)$$

$$\rho_\varepsilon = \frac{2k\varepsilon^2}{b^2} \text{ with } k = 10,\ b = \text{Burgers vector}. \quad (3)$$

Finally, the dislocation density (ρ) can be estimated by X-ray line broadening and obtained from dislocation

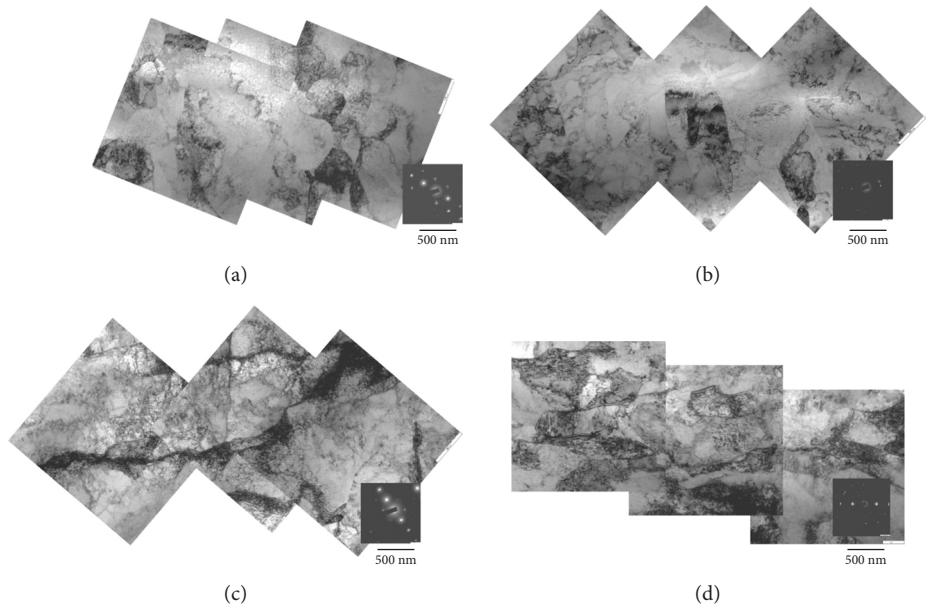

Figure 2: TEM micrographs of the SSE-processed sample: (a) two, (b) four, (c) eight, and (d) twelve passes.

densities that are related to $D \cdot (\rho_D)$ and $\varepsilon \cdot (\rho_\varepsilon)$ as follows [10]:

$$\rho = \left(\rho_D \cdot \rho_\varepsilon\right)^{1/2}. \quad (4)$$

2.4. Immersion Testing. The immersion tests were performed using the modified Livingston etchant (HCl: 30 ml; CH_3COOH: 10 ml; H_2O: 410 ml; pH = 0.41), which is known to attack dislocations and grain boundaries exclusively, leaving the other area intact [7]. The surface except the ED plane was coated with a nail lacquer to avoid a contact with the etchant solution. The immersion tests were conducted at stable room temperature condition for 1, 2, 4, 8, and 16 h. The morphology after 16 h immersion tests was observed by an optical microscope.

3. Results and Discussion

3.1. Microstructural Observation. Figure 2 shows the TEM images of the ED plane in the deformed specimens of two, four, eight, and twelve passes. After two passes, the microstructure showed a mixture of nondeformed and deformed grains with some dislocations. Up to eight SSE passes, the dislocation density increased and cell structures were observed. With increasing number of passes, the microstructure became more uniform and some grains with an average grain size of 1 μm formed. When the strain was increased through twelve SSE passes, grain size is overall constant with an average of 0.9 μm. Most interestingly, the dislocation density visible inside grains appeared to be lower than that after eight passes. The decrease in dislocation density in very high strain range after several passes in SPD was reported by Dalla Torre et al. [11], who ascribed it to the dynamic recovery during SPD.

Figure 3(a) shows the {111} peaks obtained from XRD analysis of the specimens. A significant line broadening can be observed with increasing SSE passes, which indicates a high density of dislocations and resultant long-range elastic stresses [12, 13]. The dislocation density calculated from (4) is shown in Figure 3(b) with other data estimated by direct observation by TEM [3]. The dislocation density increases gradually for two to eight passes and decreases after eight passes until twelve passes. So, the maximum dislocation density was achieved around eight passes. Though this trend is similar to the results obtained by STEM observation [3], there is a large discrepancy between two results. One possible reason for the discrepancy is that the direct observation by STEM counted only visible dislocations inside grains, whereas line broadening of XRD reflects the strain field by grain boundaries as well as discrete dislocations inside grains. Particularly, grain boundaries at nonequilibrium state are regarded as having extrinsic grain boundaries dislocations and may exert a long-range stress field [14]. Therefore, decrease in dislocation density after eight passes is associated with decease in extrinsic grain boundary dislocations, in other words, structural change from nonequilibrium to equilibrium state.

3.2. Dissolution Behavior. Figure 4 shows the weight loss of the as-annealed and SSE-processed specimens in the immersion tests in the modified Livingston etchant. The weight loss increased with increasing number of SSE passes until eight passes and decreased after twelve SSE passes. This trend was obtained for all immersion times. This result suggests that the dissolution of copper was promoted by SSE process until eight passes, but suppressed after higher passes until twelve passes.

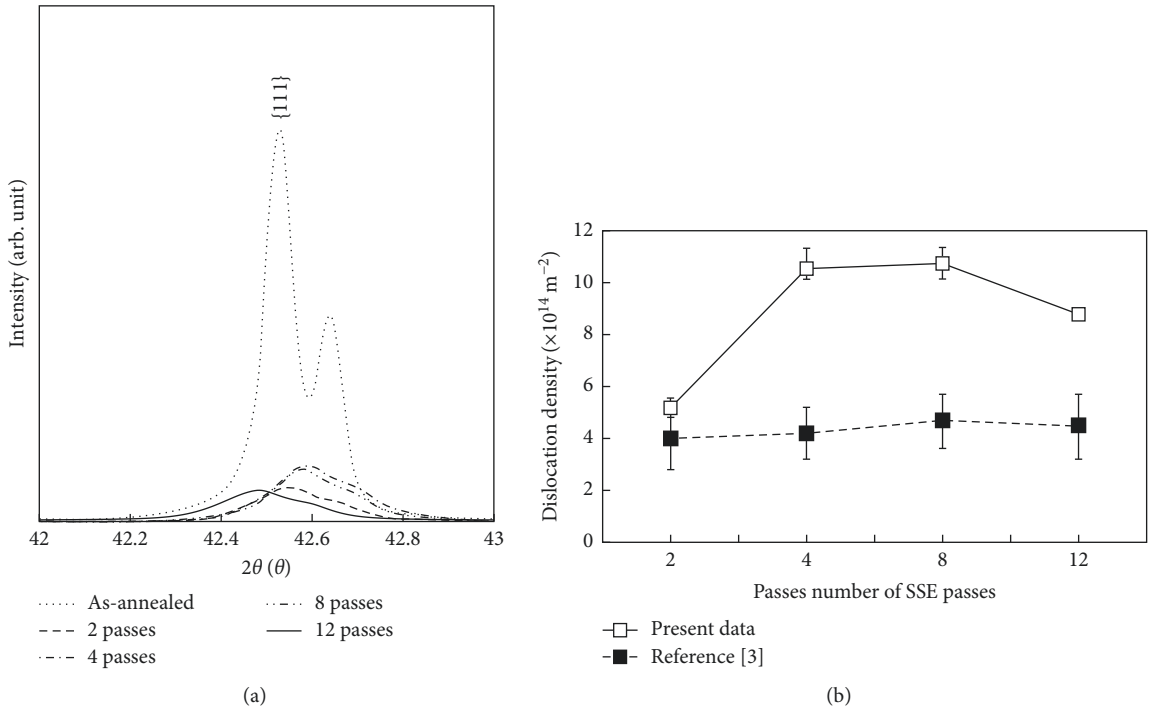

Figure 3: (a) {111} peaks of XRD patterns; (b) Dislocation density of SSE-processed sample by XRD.

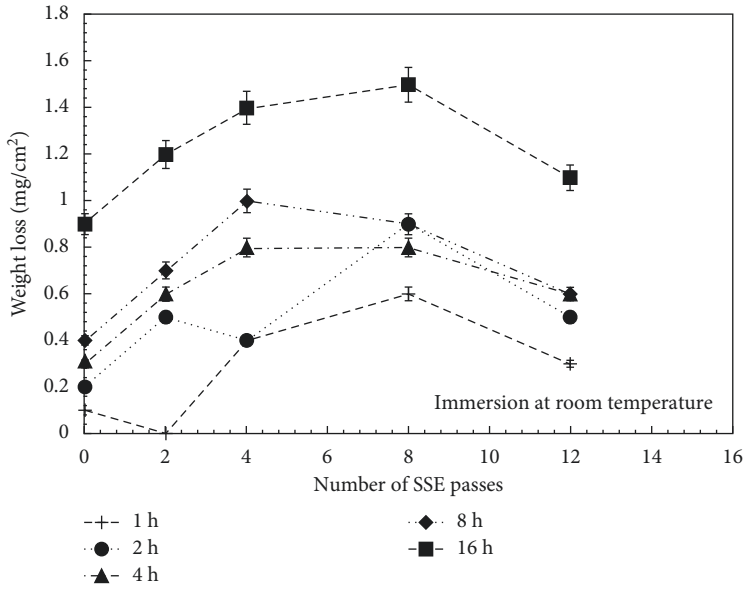

Figure 4: The weight loss of SSE-processed samples measured by the immersion tests in the modified Livingston etchant for 1, 2, 4, 8, and 16 hours.

The surface morphologies after immersion for 16 h in the Livingston etchant are shown in Figure 5. As shown in Figure 5(a), the grain boundaries groove in the as-annealed (CG) copper can be clearly observed (indicated by the red arrow), indicating that the grain boundaries were attacked predominantly while the grain interior is immune in the Livingston etchant. This is because the grain boundaries have higher energy than the grains and, therefore, work as an anode, while the grain interior works as a cathode. With increasing SSE passes and higher dislocation density, the grain boundary grooves are not visible, and the surface became smoother, as shown in Figures 5(b)–5(e). When dislocation density becomes higher than $10^{12}\,m^{-2}$, interspace between dislocations is lower than 1 μm in average, with stress field by dislocations being overlapped. Thus, dislocation pits are not isolated rending dissolution from selective to more uniform manner.

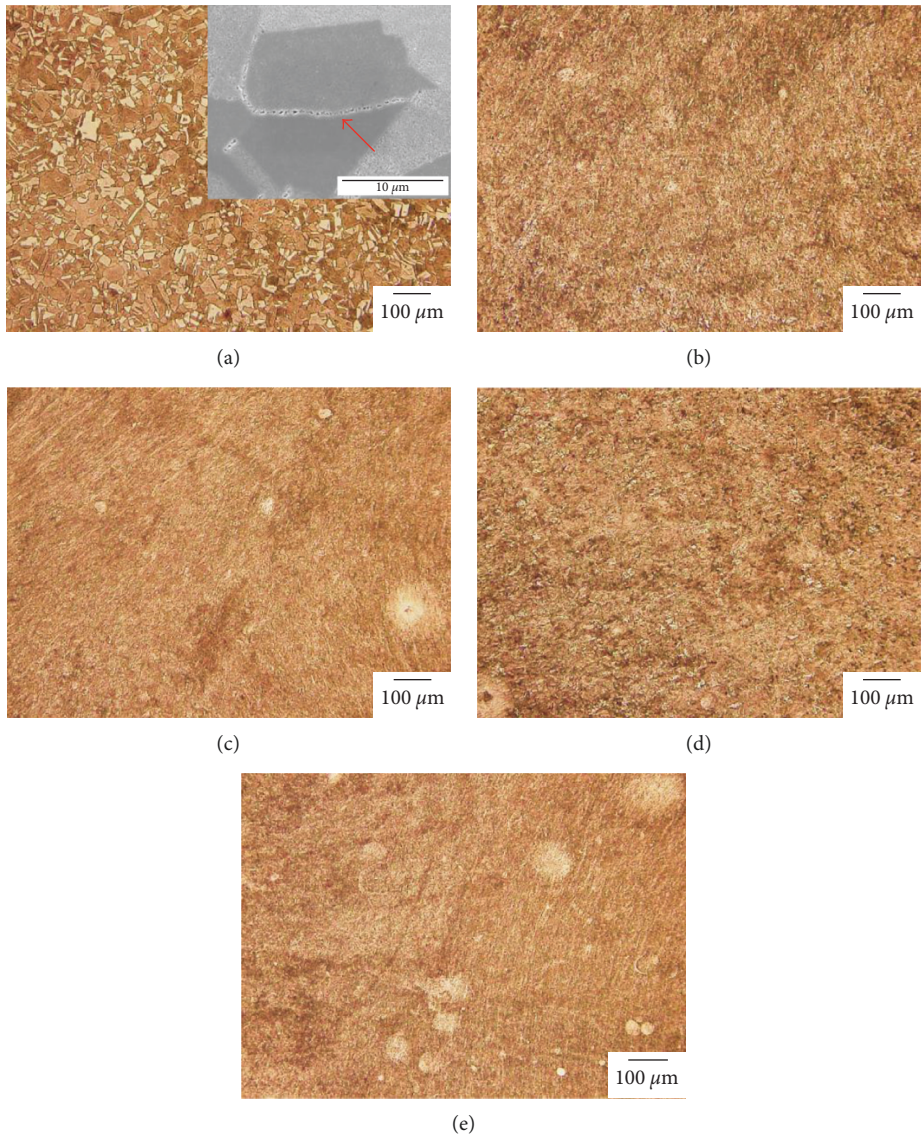

Figure 5: Dissolution surface morphology of samples: (a) as-annealed and (b) two, (c) four, (d) eight, and (e) twelve SSE passes.

The most important result in this study is that weight loss by dissolution reflects the line broadening by XRD, namely, weight loss decreases with higher strain after UFG formation. The decrease in the dislocation density after severe plastic deformation was also reported along with softening caused by the dislocation annihilation [15–21]; for example, after four passes of equal-channel angular pressing (ECAP) of pure copper, a decrease in the dislocation density was reported by Della Torre et al. [11]. According to their result, it is suggested that the decrease of stress field is also related to the operation of recovery mechanism, causing an increase in the dislocation-free grains [11]. The high extrinsic dislocation density at nonequilibrium grain boundaries may affect the dissolution rate because of lower activation energy for dissolution [4]. The dislocation annihilation inside grains as well as transition from nonequilibrium to equilibrium state therefore may cause the decreasing dissolution behavior after UFG formation in pure copper in the modified Livingston etchant.

4. Conclusions

The effect of SSE passes on the dissolution was investigated by the modified Livingston etchant which is very sensitive to dislocations. Consequently, the following major conclusions can be drawn:

(1) The internal strain field evaluated by X-ray line broadening measurements increased gradually until eight SSE passes and decreased until twelve SSE passes.

(2) The weight loss obtained by the immersion tests in Livingston dislocation etchant increased with the increasing number of SSE passes until eight passes which formed UFG and then decreased after twelve SSE passes. It reflected the variation in the internal strain obtained by XRD.

(3) The decrease in the dissolution rate may be related with the dynamic recovery, which decreases the

dislocation density inside grains and causes structural change of grain boundaries from non-equilibrium to equilibrium state.

Conflicts of Interest

The authors declare that there are no conflicts of interest regarding the publication of this paper.

References

[1] R. Z. Valiev, R. K. Islamgaliev, and I. V. Alexandrov, "Bulk nanostructured materials from severe plastic deformation," *Progress in Materials Science*, vol. 45, no. 2, pp. 103–189, 2000.

[2] N. Pardis and R. Ebrahimi, "Deformation behavior in simple shear extrusion (SSE) as a new severe plastic deformation technique," *Materials Science and Engineering: A*, vol. 527, no. 1-2, pp. 355–360, 2009.

[3] E. Bagherpour, F. Qods, R. Ebrahimi, and H. Miyamoto, "Nanostructured pure copper fabricated by simple shear extrusion (SSE): a correlation between microstructure and tensile properties," *Materials Science and Engineering: A*, vol. 679, pp. 465–475, 2017.

[4] H. Miyamoto, K. Harada, T. Mimaki, A. Vinogradov, and S. Hashimoto, "Corrosion of ultra-fine grained copper fabricated by equal-channel angular pressing," *Corrosion Science*, vol. 50, no. 5, pp. 1215–1220, 2008.

[5] J. Xu, J. Li, D. Shan, and B. Guo, "Microstructural evolution and micro/meso-deformation behavior in pure copper processed by equal-channel angular pressing," *Materials Science and Engineering: A*, vol. 664, pp. 114–125, 2016.

[6] F. W. Young Jr., "Etch pits at dislocations in copper," *Journal of Applied Physics*, vol. 32, no. 2, pp. 192–201, 1961.

[7] A. Vinogradov, T. Mimaki, S. Hashimoto, and R. Valiev, "On the corrosion behaviour of ultra-fine grain copper," *Scripta Materialia*, vol. 41, no. 3, pp. 319–326, 1999.

[8] E. Bagherpour, R. Ebrahimi, and F. Qods, "An analytical approach for simple shear extrusion process with a linear die profile," *Materials and Design*, vol. 83, pp. 368–376, 2015.

[9] E. Bagherpour, F. Qods, and R. Ebrahimi, "Effect of geometric parameters on deformation behavior of simple shear extrusion," *IOP Conference Series: Materials Science and Engineering*, vol. 63, p. 012046, 2014.

[10] K. Kapoor, D. Lahiri, S. V. R. Rao, T. Sanyal, and B. P. Kashyap, "X-ray diffraction line profile analysis for defect study in Zr-2.5% Nb material," *Bulletin of Materials Science*, vol. 27, no. 1, pp. 59–67, 2004.

[11] F. H. Dalla Torre, R. Lapovok, J. Sandlin, P. F. Thomson, C. H. J. Davies, and E. V. Pereloma, "Microstructures and properties of copper processed by equal channel angular extrusion for 1–16 passes," *Acta Materialia*, vol. 52, no. 16, pp. 4819–4832, 2004.

[12] V. Y. Gertsman, R. Birringer, R. Z. Valiev, and H. Gleiter, "On the structure and strength of ultrafine-grained copper produced by severe plastic deformation," *Scripta Metallurgica et Materiala*, vol. 30, no. 2, pp. 229–234, 1994.

[13] R. K. Islamgaliev, F. Chmelik, and R. Kuzel, "Thermal stability of submicron grained copper and nickel," *Materials Science and Engineering: A*, vol. 237, no. 1, pp. 43–51, 1997.

[14] A. A. Nazarov, "On the role of non-equilibrium grain-boundary structure in the yield and flow stress of polycrystals," *Philosophical Magazine A*, vol. 69, no. 2, pp. 327–340, 1994.

[15] K. T. Aust, U. Erb, and G. Palumbo, "Interface control for resistance to intergranular cracking," *Materials Science and Engineering: A*, vol. 176, no. 1-2, pp. 329–334, 1994.

[16] M. Yamashita, T. Mimaki, S. Hashimoto, and S. Miura, "Stress corrosion cracking of [110] and [100] tilt boundaries of α-Cu-Al alloy," *Philosophical Magazine A*, vol. 63, no. 4, pp. 707–726, 1991.

[17] W. Luo, Y. Xu, Q. Wang, P. Shi, and M. Yan, "Effect of grain size on corrosion of nanocrystalline copper in NaOH solution," *Corrosion Science*, vol. 52, no. 10, pp. 3509–3513, 2010.

[18] C. P. Gräf, U. Heim, and G. Schwitzgebel, "Potentiometrical investigations of nanocrystalline copper," *Solid State Ionics*, vol. 131, no. 1-2, pp. 165–174, 2000.

[19] M. Goerdeler and G. Gottstein, "A microstructural work hardening model based on three internal state variables," *Materials Science and Engineering: A*, vol. 309-310, pp. 377–381, 2001.

[20] F. Roters, D. Raabe, and G. Gottstein, "Work hardening in heterogeneous alloys—a microstructural approach based on three internal state variables," *Acta Materialia*, vol. 48, no. 17, pp. 4181–4189, 2000.

[21] F. H. Dalla Torre, A. A. Gazder, E. V. Pereloma, and C. H. Davies, "Recent progress on the study of the microstructure and mechanical properties of ECAE copper," *Journal of Materials Science*, vol. 42, no. 5, pp. 1622–1637, 2007.